Selectins Ligand Decorated Drug Carriers for Activated Endothelial Cell Targeting

Xavier Banquy,[†] Grégoire Leclair,[†,‡] Jean-Michel Rabanel,[†] Anteneh Argaw,[§] Jean-François Bouchard,[§,||] Patrice Hildgen,*[,†,||] and Suzanne Giasson*[,†,||,⊥]

Faculté de Pharmacie, Ecole d'Optométrie, and Département de Chimie, Université de Montréal, and Groupe de Recherche Universitaire sur le Médicament de l'Université de Montréal, C.P. 6128, succursale Centre-Ville, Montréal, Québec, H3C 3J7, Canada, and Merck-Frosst Canada, Kirkland, Québec, Canada. Received June 25, 2008; Revised Manuscript Received August 14, 2008

New active particulate polymeric vectors based on branched polyester copolymers of hydroxy-acid and allyl glycidyl ether were developed to target drugs to the inflammatory endothelial cell surface. The hydroxyl and carboxyl derivatives of these polymers allow grafting of ligand molecules on the polyester backbones at different densities. A known potent nonselective selectin ligand was selected and synthesized using a new scheme. This synthesis allowed the grafting of the ligand to the polyester polymers, preserving its binding activity as assessed by docking simulations. Selectin expression on human umbilical cord vascular endothelial cells (HUVEC) was induced with the pro-inflammatory bacterial lipopolysaccharide (LPS) or with the nonselective inhibitor of nitric oxide synthase L-NAME. Strong adhesion of the ligand decorated nanoparticles was evidenced *in vitro* on activated HUVEC. Binding of nanoparticles bearing ligand molecules could be efficiently inhibited by prior incubation of cells with free ligand, demonstrating that adhesion of the nanoparticles is mediated by specific interaction between the ligand and the selectin receptors. These nanoparticles could be used for specific drug delivery to the activated vascular endothelium, suggesting their application in the treatment of diseases with an inflammatory component such as rheumatoid arthritis and cancer.

INTRODUCTION

Inflammation is a naturally occurring defense mechanism upon exposure to specific antigens, chemicals, infections, and physical stress. It is characterized by different events taking place at or near the injured area, including vascular endothelium cell (VEC) activation and leukocyte accumulation. VEC, upon activation by pro-inflammatory cytokines, increases the expression of cell adhesion molecules (CAMs) in a highly regulated and sequential process. This sequence involves expression of P-selectin followed by E-selectin, which promote rolling and tethering of leukocytes along the vessel wall (*1*). Exaggerated and/or prolonged inflammatory response is associated with a large number of acute and chronic disorders, including organ ischemia/reperfusion injury, allergic asthma, rheumatoid arthritis, inflammatory bowel disease, and atherosclerosis.

The selectin family has three members, namely, L-, E-, and P-Selectin. Their expression is restricted to circulating leukocytes (L-selectin) and VEC (P- and E-selectins). Upon inflammatory stimulation, P-selectin (CD62P) appears rapidly at the cell surface, owing to its intracellular storage in Weibel-Palade bodies. On the other hand, maximum levels of E-selectin (CD62E) are reached in 4−6 h after activation, due to *de novo* synthesis (*2*). Since E-selectin is expressed in both acute and chronic inflammation, it has been considered as a good candidate for drug targeting. In addition, the cytokines IL-1β and TNFα, as well as bacterial lipopolysaccharide (LPS), have been shown to stimulate the expression of E-selectin (*3*). Moreover, E-selectin is reported to exhibit a highly localized expression in neovasculature (*4*) and prostate cancer (*5*). The natural ligands of E- and P-selectin are either fucosylated glycoproteins (ESL-1, for E-selectin ligand) or sialomucin glycoproteins (PSGL-1 for P-selectin glycoprotein-1) presenting sialylated carbohydrate moieties (sialyl-Lewis x, sLe^x) epitopes. These selectin ligands are known to be present on circulating leukocytes plasmatic membrane (*6, 7*). Synthetic analogues of the natural ligands have been investigated for their ability to block inflammation (*6, 8, 9*). Some of these analogues have been reported to have higher affinity to the target compared to the natural ligand, rendering them very attractive molecules for active drug targeting developments.

Among promising new therapeutic approaches, targeted drug carriers have received increasing interest during the past few decades (*10*). These carriers aim to release the drug close to the pathologic site, protecting the active substance from fast degradation and elimination leading to dose reduction and avoiding side effects. Several approaches such as drug immunoconjugation, bioconjugation, liposomes, dendrimers, micelles, or coated nanoparticles (NPs) have been proposed to achieve active or passive targeting of drug. However, compared to other delivery systems, polymeric NP drug carriers offer the possibility of encapsulating several types of molecules and protecting them from enzymatic degradation. The polymers forming the NP carriers are generally highly stable in physiological media and allow controlled release by matrix degradation.

A general approach to confer targeting capabilities to NPs is to functionalize their surface with a specific ligand. This approach is strongly limited by the stability of the link between the ligand and the NP surface. If this link is not stable enough in physiological media, release of the ligand (by hydrolysis, for example) from the NP surface could be rapid. To circumvent

* To whom correspondence should be addressed: patrice.hildgen@umontreal.ca; suzanne.giasson@umontreal.ca.
[†] Faculté de Pharmacie, Université de Montréal.
[‡] Merck-Frosst Canada.
[§] Ecole d'Optométrie, Université de Montréal.
[||] Groupe de Recherche Universitaire sur le Médicament de l'Université de Montréal.
[⊥] Département de Chimie, Université de Montréal.

10.1021/bc800257m CCC: $40.75
Published on Web 09/20/2008

Scheme 1. Chemical Structure of the Synthetic Ligand of E- and P-Selectin

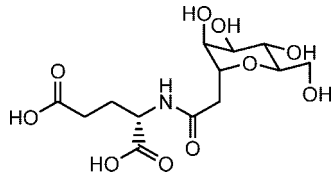

this severe drawback and to improve the binding properties of the NPs, new coupling strategies must be investigated.

Specific drug delivery to activated VECs to modulate the inflammation response have been shown to be a valid therapeutic strategy (*11*). Drug immunoconjugation (*12, 13*) and immunoliposomes directed against E-selectin (*14*−*16*), as well as liposomes incorporating sLe^x as ligands (*17*−*19*), are among the most described methods. They all present the strong disadvantage of using natural ligands (as sLe^x) which are in competition with the free homologue in the bloodstream.

In this study, a ligand of E- and P-selectin was synthesized and conjugated to a poly-L,D-lactic acid polymer (PLA). The ligand is a nonselective selectin antagonist, which may be advantageous in pathological settings involving both P- and E-selectin activities. The conjugation was done using carboxylic acid functions introduced in the PLA backbone. This functionalized polymer was subsequently mixed with pure PLA to form the NPs. NPs formulated with ligand functionalized PLA (NP-L) present higher adhesive capabilities to HUVEC plasmatic membrane compared to nonfunctionalized PLA NPs. Inhibition of binding could be observed for NP-L when cells are incubated with free ligand prior to the NP introduction. This study provides strong evidence that NPs functionalized with the synthetic ligand can specifically bind to endothelial cells activated by pro-inflammatory molecules.

EXPERMENTAL PROCEDURES

Materials. Chemicals were purchased from Sigma-Aldrich (Oakville, ON, Canada). Solvents were from Laboratoire MAT (Québec, PQ, Canada). All media and reagents for cell culture were purchased from Gibco (Invitrogen, Burlington, ON, Canada). Human vascular endothelial cells (CRL 1730) were from ATCC; Raw 264.7 murine macrophage cell line was a gift from Pr. J. C. Leroux.

Ligand Docking Simulations. All simulations were performed with E-selectin receptor using GOLD (Genetic Optimisation for Ligand Docking) docking program (*20*) in order to identify the most probable conformation of the free and grafted ligand interacting with its receptor. The structure of the chosen ligand can be seen in Scheme 1. The protein data file was obtained from the structure published by Somers et al. (*21*). The protein was prepared as described by Jones et al. (*20, 22*). The ligand and grafted ligand (Scheme 1 and compound (**9**)) were built using Material Studio software (Accelrys, San Diego, USA) and their structure was minimized using the Discover module assigning CFF force field to each atom. The grafted ligand consisted of a ligand molecule linked to a PLA chain (of 4 monomers) via a glycidyl linker. For the docking simulations, the binding pocket of E-selectin was defined using the conformation of the natural ligand sialyl Lewis acid X (sLe^x) given by Somers et al. The two equatorial hydroxyl groups of the mannose ring of the studied ligand were constrained to bind the calcium ion present in the binding pocket. In that way, the mannose ring of the ligand overlaid onto the L-fucose ring of the sLe^x and the glutamate side chain was free to bind to the protein amino acids. More than 30 genetic algorithm runs were performed in order to identify best fitting structures. The final optimized conformations were picked using GOLD scoring function.

Scheme 2. General Synthesis of the Selectin Ligand

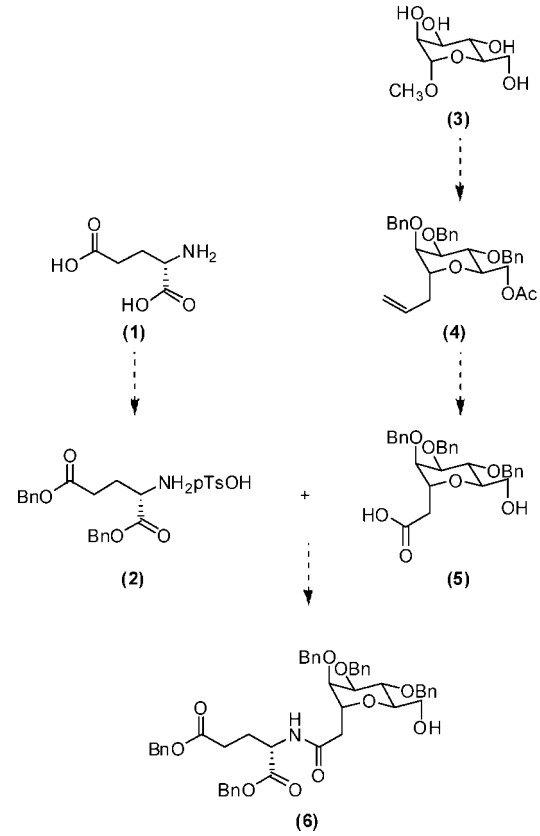

Ligand Synthesis. A general scheme of the ligand synthesis is represented in Scheme 2.

*Synthesis of Fragment **2**.* 25.5 g of *p*-toluene sulfonic acid (*p*TsOH) were added to a solution of 10 g glutamic acid **1** in 100 g of benzylic alcohol under N_2 atm. The mixture was heated at 80 °C for 24 h under stirring and subsequently poured onto 1 L aqueous solution of 1 M NaOH and extracted three times with diethyl ether (Et_2O). The organic phases were pooled and dried on Na_2SO_4. A solution of 10 g (*p*TsOH) sulfonic acid (*p*TsOH) in 100 mL Et_2O was added to the organic phase, which was kept at 4 °C for 24 h. The crystals obtained were filtered and washed with ether to yield 12.3 g of product **2** (36% yield).

^{1}H NMR (400 MHz, DMSO-d_6) δ 2.00−2.17 (m, 2 H, -CH_2−CH_2−CH-), 2.28 (s, 3 H, CH_3- (*p*TsO^-)), 2.43−2.66 (m, 2 H, -CH_2−CO_2Bn), 4.17 (t, 6.60 Hz, 1 H, -CH(NH_3^+)-CO_2-), 5.05−5.12 (m, 2 H, -CH_2−Ph), 5.17−5.26 (m, 2 H, -CH_2−Ph), 7.12 (d, 8.0 Hz, 2 H, aromatic *p*TsO^-), 7.31−7.43 (m, 10 H, aromatic -Bn), 7.51 (d, 8.0 Hz, 2 H, aromatic *p*TsO^-), 8.28−8.64 (m, 3 H, -NH_3^+). SM (FAB) *m/e* 328.5 (M + H-*p*TsOH, 100%), 192.3 (10%), 154.2 (32%).

*Synthesis of Fragment **4**.* 3.8 g of tetrabutyl ammonium iodide (TBAI) and 54 mL of bromobenzyl (BnBr) were added to a 10% (w/w) solution of α-methylmannoside **3** in dimethyl formamide (DMF) under N_2 atmosphere. The mixture was cooled down to 0 °C and 18.2 g of NaH was slowly added to avoid a temperature rise. The mixture was stirred for 16 h and cooled down to 0 °C. 100 mL of isopropanol was slowly added, followed by 20 g of salicylic acid. The solution was evaporated and redissolved in 500 mL of ethyl acetate (EtAc). The organic phase was washed three times successively with 100 mL NaOH 10%, 100 mL 1 N HCl, and 100 mL NaCl saturated salt solutions. The organic phase was dried on Na_2SO_4, filtered, and evaporated. The residual product was purified by flash chromatography on silica with an eluent mix 10:90 to 20:80 Et_2O and hexane (HEX) to yield 27.3 g (43%) of intermediate product.

^{1}H NMR (400 MHz, $CDCl_3$) δ 3.35 (s, 3 H, -OCH_3), 3.74−3.84 (m, 4 H), 3.90−3.93 (m, 1 H), 3.97−4.04 (m, 1 H), 4.51−4.82 (m, 8 H), 4.91 (d, 11.0 Hz, 1 H), 7.17−7.42 (m, 20 H, aromatic). ^{13}C NMR (400 MHz, $CDCl_3$) δ 54.7, 69.2, 71.6, 72.0, 72.5, 73.3, 74.4, 74.8, 75.0, 80.2, 98.9, 127.4−128.4 (m, 20 C), 138.2−138.4 (m, 4 C). SM (FAB) *m/e* 553.4 (M − H, 7%), 271.4 (10%), 181.3 (100%). SMHR Calculated for $C_{35}H_{37}O_6$ (M − H) 553.2590, found 553.2600 (−1.8 ppm).

Allyltrimethylsilane (14.3 mL) and trimethylsilyl triflate (4.1 mL) were added to a solution of 25 g of intermediate product in acetonitrile (ACN) at 0 °C under N_2 atmosphere. The mixture was maintained at 4 °C for 16 h, and then 65 mL of anhydrous acetic acid was added. Under stirring at room temperature, 600 mL of dichloromethane (DCM) and 60 mL of aqueous solution of $NaHCO_3$ were added to the mixture. The pH was adjusted to 12 with 10% w/v NaOH. After phase separation, the aqueous phase was extracted with 300 mL of DCM. The obtained organic phases were pooled, dried on Na_2SO_4, and filtered. The solvents were eliminated by distillation under vacuum. The residual product was purified by flash chromatography on silica, using a mix of Et_2O and HEX in proportion ranging from 25:75 to 100:0 to yield 18.5 g (79%) of product **4**.

^{1}H NMR (400 MHz, $CDCl_3$) δ 2.05 (s, 3 H, Ac-), 2.24−2.40 (m, 2 H), 3.61−3.64 (m, 1 H), 3.75−3.83 (m, 3 H), 4.05−4.10 (m, 1 H), 4.23−4.27 (m, 1 H), 4.37−4.42 (m, 1 H), 4.53−4.63 (m, 5 H), 4.74−4.77 (m, 1 H), 4.99−5.04 (m, 2 H), 5.67−5.77 (m, 1 H), 7.27−7.37 (m, 15 H, aromatic).

Synthesis of Fragment ***5***. 90 mL water and 4.5 mL of an aqueous solution of 50% (w/w) of 4-methylmorpholine *N*-oxide (NMO) were added to a solution of 9.00 g of compound **4** in 90 mL distilled acetone, followed by an addition of 2.25 mL of a 2.5% (w/w) solution of osmium tetraoxide in *t*-butanol. The solution was stirred for 3 h; then, 2.25 mL of an aqueous solution of 10% (w/w) $Na_2S_2O_3$, 9 g of Florisil, and 180 mL of water were added. The pH was adjusted to 1 with 1 M HCl. The aqueous phase was extracted three times with 500 mL of EtAc. The organic phases were pooled, dried on Na_2SO_4, and filtered. The solvent was eliminated by distillation under vacuum. The diol intermediate product was used in the next step without purification. 4.5 g of sodium periodate and 90 mL of water were added to a solution of 17.4 mM of the intermediate diol in 90 mL THF. The solution was stirred for 1 h and then 450 mL of water was added. The aqueous phase was extracted three times with 450 mL of EtAc. The organic phases were pooled, dried on Na_2SO_4, filtered, and the solvent eliminated by distillation under vacuum. The residual aldehyde product was used in the next step without further purification. 20.9 mM of CrO_3 from the Jones reagent (CrO_3:H_2SO_4:H_2O, 1:1:3) were added to a solution of 17.4 mM of aldehyde product in 90 mL of distilled acetone at 0 °C. After 15 min, reagent in excess was neutralized by the addition of 10 mL of isopropanol. The solution was poured on 900 mL of 1 M HCl and extracted three times with 400 mL of EtAc. The organic phases were pooled, and the remnant solvent was eliminated by distillation under vacuum. The aldehyde product was used in the next step without further purification. A solution of 4.0 g potassium hydroxyde was prepared with 20 mL water and 20 mL of MeOH. This solution was added to a solution of 17.4 mM of intermediate aldehyde compound in 100 mL MeOH. 100 mL of potassium hydroxyde 10% (w/v) was further added and the mixture poured into 1 L of 1 N HCl; then, the aqueous phase was extracted three times with 500 mL EtAc. The organic phases were pooled, dried on Na_2SO_4, filtered, and the solvent eliminated by distillation under vacuum. The residual product was purified by flash chromatography on silica using Et_2O as the eluent to obtain 7.56 g of acid alcohol **5**. The yield of the synthesis was 88%.

^{1}H NMR (400 MHz, $CDCl_3$) δ 2.54 (dd, 9.9 and 16.7 Hz, 1 H), 2.82 (dd, 3.3 and 16.8 Hz, 1 H), 3.45 (dd, 3.7 and 12.1 Hz, 1 H), 3.55 (dd, 3.6 and 5.0 Hz, 1 H), 3.62 (dd, 2.8 and 7.6 Hz, 1 H), 3.81 (dd, 3.0 and 5.0 Hz, 1 H), 3.84−3.92 (m, 1 H), 4.21 (dd, 9.1 and 12.2 Hz, 1 H), 4.39−4.59 (m, 7 H), 7.22−7.38 (m, 15 H), -OH and -COOH absent. SM (FAB) *m/e* 515.2 (M + Na, 4%), 271.1 (8%), 181.1 (100%), 132.9 (51%). SMHR Calculated for $C_{29}H_{32}O_7Na$ (M + Na) 515.2046, found 515.2032 (+2.7 ppm).

Coupling ***2*** *and* ***5****: Protected Ligand* ***6***. 9.5 g of amine tosylate **2** was solubilized in 200 mL of EtAc and mixed three times with the same volume of 1 N NaOH. The amine compound corresponding to **2** was obtained after drying the organic phase on Na_2SO_4 and filtration and elimination of the solvent by evaporation under vacuum. A 10% (w/w) solution of the acid alcohol **5** in DCM was added with a canula to a solution containing 2.4 g of ethyl-3-(3-dimethylaminopropyl)-carbodiimide (EDC). 1.7 g of 1-hydroxybenzotriazole hydrate (HOBt) and compound **2** were mixed in 31 mL DCM under N_2 atmosphere. The solution was stirred for 16 h. Solvents were eliminated by distillation under vacuum. The residual product was purified by flash chromatography on silica using 1:1 EtAc/HEX to get 3.17 g of the protected ligand **6** (yield of 63%).

^{1}H NMR (400 MHz, $CDCl_3$) δ 1.92−2.02 (m, 1 H), 2.14−2.23 (m, 1 H), 2.31−2.45 (m, 3 H), 2.69 (dd, 2.0 and 15.4 Hz, 1 H), 3.40 (dd, 3.0 and 12.3 Hz, 1 H), 3.50 (dd, 3.0 and 4.8 Hz, 1 H), 3.57 (dd, 2.6 and 8.2 Hz, 1 H), 3.78 (dd, 3.1 and 4.4 Hz, 1 H), 3.96−4.01 (m, 1 H), 4.26 (dd, 9.9 and 12.4 Hz, 1 H), 4.33−4.40 (m, 1 H), 4.43−4.61 (m, 6 H), 4.67−4.74 (m, 1 H), 5.05 (d, 12.3 Hz, 1 H), 5.09 (d, 12.4 Hz, 1 H), 5.14 (s, 2 H), 7.15−7.39 (m, 25 H), -OH and -CONH- absent. ^{13}C NMR (400 MHz, $CDCl_3$) δ 27.07, 30.28, 37.27, 51.49, 59.92, 66.51, 67.50, 71.52, 72.47, 72.83, 74.69, 75.72, 76.89, 127.76−128.60 (25 °C), 134.98, 135.66, 137.63, 137.68, 137.78, 171.20, 172.51, 172.70. SM (FAB) *m/e* 802.2 (M + H, 68%), 694.3 (10%), 418.2 (8%), 328.1 (12%), 271.1 (6%), 181.1 (100%), 136.0 (14%). SMHR Calculated for $C_{48}H_{52}NO_{10}$ (M + H) 802.3591, found 802.3554 (+4.6 ppm).

Polymer Synthesis and Subsequent Ligand Conjugation and Deprotection. Synthesis of PLA polymer bearing pendant carboxyl groups for ligand grafting has been described elsewhere (*23*). A solution of PLA 1 mg/mL with 1% (mol/mol) (relative to lactic monomer) acyl chloride pendant groups in chloroform was prepared (polymer **7**) and to this were added successively 1.5 equiv of **6** in chloroform at a concentration of 0.25 mM and a 10% (w/v) solution of dimethylamino propane (DMAP) in pyridine. The mixture was stirred for 3 h after which a 1 N HCl solution was added to neutralize the pyridine. Chloroform was evaporated and the aqueous phase was filtered to yield the protected ligand−PLA. Activated palladium (Pd−C 5%) was added to a solution of 0.8 mg/mL of protected ligand−polymer in glacial acetic acid at a ratio of 1 mg/mg. This mixture was placed under hydrogen (atmospheric pressure) for 16 h. Pd−C was eliminated by filtration on Celite (MeOH as eluent). Solvent was eliminated by evaporation, and the product dissolved in chloroform. Chloroform was eliminated by evaporation in the presence of an equivalent volume of water to yield the precipitated polymer in aqueous phase. This step was repeated twice to obtain PLA with 5 mol % of grafted selectin synthetic ligand (compound **9** or PLA-$SEL_{5\%}$) with a 70% yield for the two-step procedure after drying.

PLA polymer bearing hydroxyl groups was synthesized as described in Nadeau et al. (*23*). Rhodamine B was grafted to the PLA backbone using standard EDC/NHS coupling reaction. The obtained polymer (PLA-$Rhod_{5\%}$) was precipitated in water and dissolved in DCM after complete water removal. This

operation was repeated three times for complete elimination of remnant chemicals.

NP Preparation. NPs were prepared by the solvent evaporation method. Briefly, 500 mg of a 1:1 mixture of PLA-$Rhod_{5\%}$ and PLA (or PLA-$Sel_{5\%}$) were dissolved in 15 mL of DCM. The polymer solution was then gently injected into 100 mL of aqueous 15% (w/v) of sucrose solution containing a surfactant mixture (2.5% Tween 20, 0.5% PEG Laurate), while emulsification was being achieved by means of high-pressure homogenization (Emulsiflex C30, Avestin, Ottawa, ON, Canada) at 10 000 psi for 3 min in order to obtain the NP suspension. After collection of the NPs, the suspension was stirred for 5 h under reduced pressure to allow solvent evaporation and NP solidification. NP suspension was then lyophilized (Freeze-Dry System, Lyph.Lock 4.5, Labconco) and stored at 4 °C until further use.

NP Characterization. *Particle Size Distribution.* NP size distribution was measured by photon correlation spectroscopy (PCS) (N4 Plus, Coulter Electronics, Miami, FL) at 90° scattering angle for 180 s and at 25 °C. The mean particle diameter was calculated using differential size distribution processor (SDP) intensity analysis program.

Zeta Potential Measurements. NPs were suspended in 0.25% (w/v) saline solution filtered through 0.22 μm filter and zeta potential was measured at 25 °C on a Malvern ZetaSizer Nanoseries ZS (Malvern Instruments, Worcestershire, UK) in triplicate.

Time-of-Flight Secondary Ion Mass Spectrometry (TOF-SIMS). NP samples were analyzed using a TOF-SIMS IV (ION-TOF GmbH, Munster, Germany). The mass spectra were produced by irradiating the NPs with a 15 keV monoisotopic $^{69}Ga^+$ primary ion source with a target current of 1.02 pA in order to stay in static regime (ionic dose lower than 10^{13} ions/cm^2). Mass resolution was above 8200 μma for $^{29}Si^+$. The scanned surface area was 40 μm × 40 μm. Both positive and negative secondary ions were collected over a mass range 5−800 and analyzed.

Cytotoxicity Assay of NPs. Cytotoxicity assay was performed on two cell lines using MTT cell proliferation assays. RAW 264.7 murine macrophage cell line was cultured in Dulbecco's Modified Eagle Medium (DMEM) supplemented with 10% fetal bovine serum (FBS) and penicillin/streptomycin (Invitrogen Canada, Burlington, ON, Canada). Human vascular endothelium cells were cultivated in F12 Kaighn's modification medium, 10% FBS with penicillin/streptomycin supplemented with heparin, and endothelial growth supplement from neural bovine tissue (Sigma-Aldrich, Oakville, ON). Both cell lines were grown in tissue culture flasks and incubated at 37 °C in a 5% CO_2 atmosphere.

Raw 264.7 cells were diluted in complete medium at a final concentration of 5×10^5 cells/mL and plated (100 μL/well) on a 96 well flat-bottom microplate (Corning, NY). NPs suspended in 10 μL PBS sterile buffer were added in the wells in triplicate for each concentration. The plates were incubated for 24 h after which cellular proliferation was assessed by MTT assay. Cell medium was removed and cell monolayer washed with PBS. Complete medium was replaced and 10 μL of thiazolyl blue tetrazolium bromide (Sigma-Aldrich, Oakville, ON, Canada), dissolved in PBS (10 mM, pH 7.4) at a concentration of 5 mg/mL and filtered on 0.22 μm sterile filter (Millipore, Bedford, MA), was added to each well. After 3 h incubation time at 37 °C in 5% CO_2 atmosphere, 50 μL of solubilizing solution (Isopropanol, 10% Triton X100, 0.1 N HCl) was added to each well to dissolve the dark blue formazan crystals. Absorbance was read at a wavelength of 570 nm on a microplate reader (SAFIRE, Tecan, Austria). Procedures with HUVECs were similar, except for initial seeding densities of 2×10^4 cell/m were plated on 96 well flat-bottom microplate (treated with fibronectin) and extra incubation time of 6 h was used prior to addition of solubilizing solution.

***In Vitro* Binding Assays.** *Selectin Induction by Pro-Inflammatory Drugs.* HUVEC were plated on sterile round coverslips (Fisher Scientific, Ottawa, ON, Canada) treated with human fibronectin at a seeding density of 5×10^4 cells/wells and grow for 48 h prior to experiment in 24 well plates (Costar, Corning). Selectin expression on the cell surface was induced by LPS (5 μg/mL) or with L-NAME (3 mM) for 4 h. After repeated rinsing with cold PBS, the activated cells were fixed with a filtered 1% (w/w) formaldehyde PBS solution for 10 min. After addition of 250 μL of blocking solution (2% (w/v) BSA in PBS), cells were incubated overnight at 4 °C with mouse anti-E-Selectin (clone BBIG-E4 (5D11), R&D Systems, Minneapolis, MN) or P-Selectin (clone P8G8, Chemicon, Temecula, CA) antibodies. After washing with PBS, secondary goat antimouse Alexa546 antibody (Invitrogen) was added for 2 h. Cell nucleus staining was performed using Hoechst 33352. All micrographs were taken using an inverted Olympus IX71 microscope (Olympus Canada Inc., Markham, ON) and an Evolution VF camera (MediaCybernetics, Bethesda, MD) with the same 60× objective lens and exposure time to allow comparison of measurements. All images were processed with ImagePro software (MediaCybernetics, Bethesda, MD).

NP Binding Assays. HUVECs were activated as described above and cooled to 4 °C prior to incubation with cold NP suspension for 5 min (100 μg/wells) in serum-free medium. After repeated rinsing with cold PBS, cells were lysed for 2 h at 2 °C with a 0.2% (w/w) Triton X100 solution (1 N NaOH), and fluorescence intensity was read with a fluorescence plate reader (Ex., 550 nm; Em., 580 nm). A similar procedure was used for studies using the free ligand as an inhibitor. Activated HUVECs were incubated for 30 min at 37 °C with different concentrations of free ligand and cooled to 4 °C before incubation with NPs (50 μg/mL) in serum-free medium. After repeated rinsing with cold PBS, cells were lysed during 2 h and fluorescence was read at 25 °C.

Statistical Analysis. The data were calculated as means ± SE, where statistical significance was determined by Student's *t* test.

RESULTS

Ligand Docking Simulations. The synthetic ligand (see Scheme 1), an analogue of the sLe^x epitope, was selected in this study due to its high binding affinity for P- and E-selectin (*8*) compared to sLe^x (*9*). Ligand docking simulations were performed on E-selectin in order to confirm that grafted ligands still possess high binding affinity to receptors. The synthetic ligand is a mannose-based mimic of sLe^x, whose structure incorporates a carboxylate group which replaces the Gal residue. Interaction between sLe^x and E-selectin has been extensively described and is now well-understood. The binding site of E-selectin is known to be located on the lectin domain of the protein. The calcium ion present in this domain has two main functions: to maintain the structure of the binding site (the calcium ion interacts with 5 residues of the protein, namely, Glu80, Asn82, Asn83, Asn105, and Asp106) and to bind the two hydroxyl groups in the equatorial position of the l-fucose ring of the sLe^x ligand. This last function has been extensively used to develop ligands derived from mannose and having two hydroxyl functions in the equatorial position and another one in the radial position.

Results from docking simulations performed with the synthetic ligand showed that the mannose cycle fits in the binding site and interacts strongly with a large number of amino acids forming the binding pocket. One of the two equatorial hydroxyl functions of the mannose ring was able to bond strongly to the

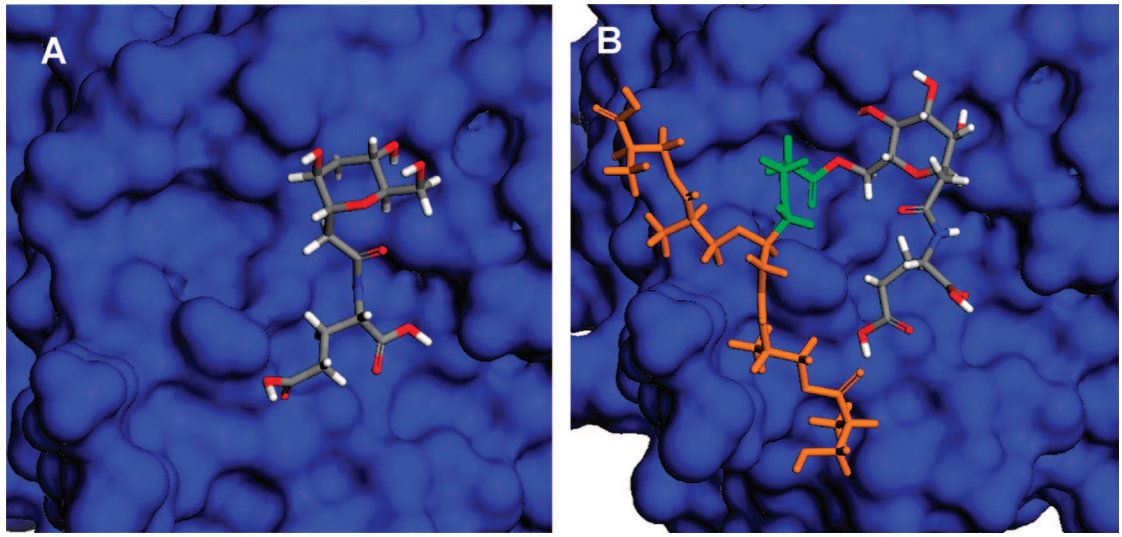

Figure 1. Conformation of the ligand in the bonded state obtained from docking experiments. (A,B) Top view of the binding pocket. Protein is represented by the Connelly surface in blue. The PLA is chain represented in orange. Linker monomer is represented in green.

Scheme 3. Grafting Reaction of the Synthetic Ligand on a PLA Chain and Deprotection

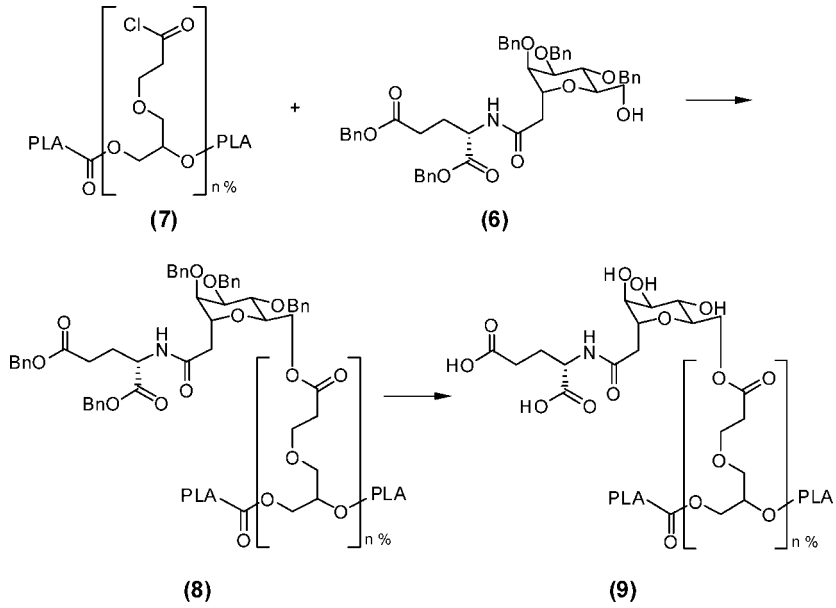

calcium ion of the lectin domain, while the other one interacted with Asp106 and Asn83 side chains. Moreover, one carboxylate of the glutamate moiety of the ligand binds strongly to Arg97 and to Tyr48. These interactions allow the ligand to be positioned in a similar direction to sLe^x. It is interesting to note that the synthetic ligand interacts with the same amino acid as sLe^x but with almost no steric constraint, which is certainly the cause of its potent inhibition capacity. Moreover, these docking simulations showed that one hydroxyl group of the mannose ring is not involved in the binding pattern and could be used as a coupling function with a macromolecule.

We performed another series of docking simulations using the synthetic ligand grafted to a PLA chain of 5 monomers. The interaction pattern of the grafted ligand was very similar to the original nongrafted ligand. We observed that the fitness index of the best structure was much higher for the grafted ligand than for the nongrafted ligand, indicating that the presence of the polymer chain favored binding of the ligand. The conformations of the free and grafted ligands in the binding pocket are slightly different. One remarkable difference is the position of the mannose ring, which is flipped in the case of the grafted ligand (Figure 1). This conformational change allows the polymer chain to lie aside from the binding pocket. Surprisingly, this conformation does not affect the interaction pattern of the ligand. The hydrogen bond network between the receptor and the grafted ligand was identical to that of the free ligand. The same amino acids from the receptor were involved in the interaction pattern as well as the same hydroxyl groups from the mannose ring and the carboxylate groups from the glutamate moiety of the ligand. The main difference between the two interaction patterns is located in the two hydroxyl groups of the mannose ring, which are inverted in the case of the grafted ligand compared to the free ligand configuration.

Table 1. Particle Size and Zeta Potential Measurements of the Different NPs Used in This Study

tested nanoparticles	particle size (nm)	zeta potential (mV)
PLA-Rhod/PLA-SEL5%	173 ± 23	−25.7
PLA-Rhod/PLA	168 ± 37	−19.2

Ligand and Polymer Synthesis. Protected ligand **6** was obtained from the coupling between the amine of the protected

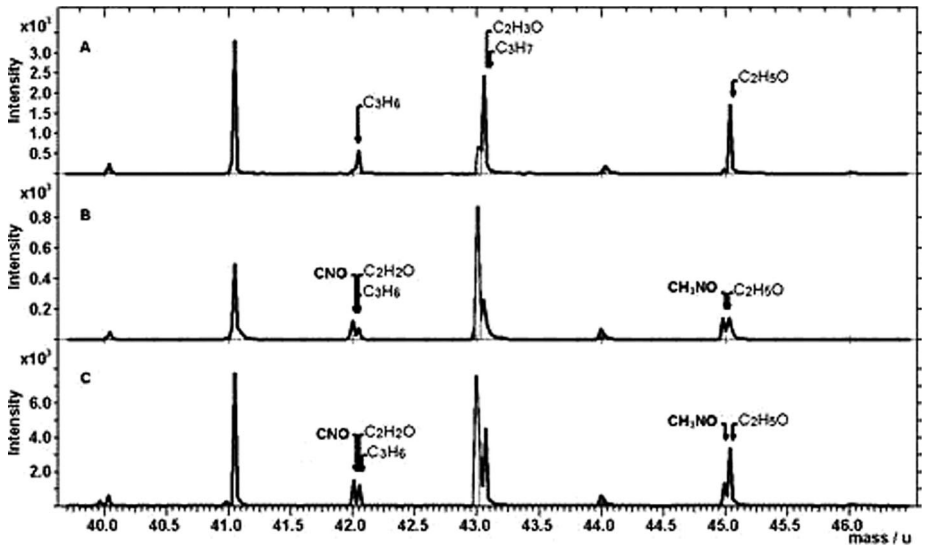

Figure 2. Partial TOF-SIMS spectrum (40−46 amu). (A) NPs made of PLA, (B) NPs made of PLA and PLA-SEL$_{5\%}$ (50:50), and (C) NPs made of PLA-SEL$_{5\%}$ alone. Significant peaks are identified by arrows.

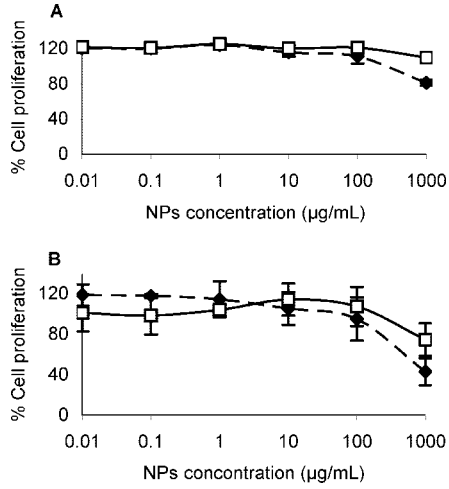

Figure 3. Cytotoxicity assays of NPs on endothelial cells and rat macrophages. (A) NPs suspended in PBS were incubated with Raw 264.7 murine macrophage cell line; (B) NPs were incubated with HUVEC. □, NPs bearing the synthetic ligand; ♦, NPs made of PLA only.

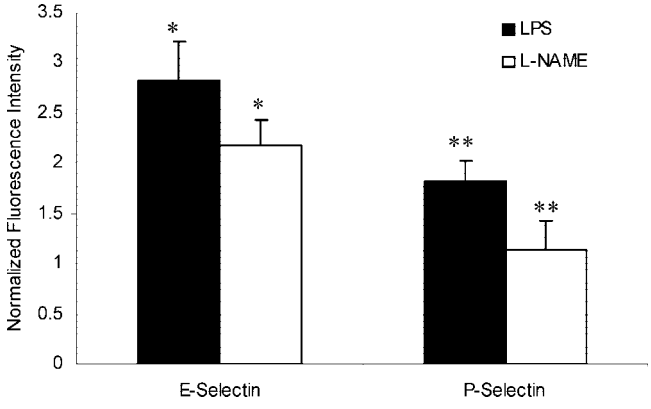

Figure 4. Normalized E- and P-selectin expression quantification from fluorescence microscopy in response to LPS and L-NAME activation ($p < 0.01$, $n = 3$). Fluorescence intensity per cell was quantified and normalized to basal expression.

amino acid **2** and the acid **5** (Scheme 2). A challenging aspect of this reaction was to realize the coupling in the presence of free hydroxyl functions on **5**. The reaction sequence was important in order to prevent oxidation of the primary hydroxyl groups into carboxylic acid. We used acetyl functions to protect the primary alcohol during the reaction. As illustrated in Scheme 3, the coupling reaction yielded the amide ligand **6** ready to be grafted to PLA. The grafting of the synthetic ligand to PLA was mediated by an ester linkage on pendant groups of a new family of polyester polymers developed in our laboratory (*23*). For this purpose, the ligand must present only one reactive hydroxyl group, which does not belong to the active part of the ligand. The use of a benzyl group to protect the other hydroxyl and carboxyl functions was guided by the ease of removal by hydrogenation in one step after polymer grafting. The presence and removal of the benzyl group before and after deprotection of the grafted ligand was confirmed by NMR (data not shown). The ligand grafting reaction takes place between the unprotected hydroxyl group on the ligand **6** and the acyl chloride groups present on the polymer pendant groups **7** in the presence of DMAP and pyridine (Scheme 3). Molecular weights of the synthesized polymers, determined by GPC, were found to be M_n 23 103, M_w 41 623 for PLA and M_n 16 412, M_w 34 868 for PLA-SEL$_{5\%}$. A small decrease of the molecular weight of PLA-SEL$_{5\%}$ could be due to partial hydrolysis of the polymer, as some reaction steps of the ligand grafting reaction involve acidic or basic treatments. The free ligand was obtained by catalytic hydrogenation of **6**, which removed the benzyl protecting groups and gave the ligand described by Wong et al. (*8, 24*). The structure of the free ligand was confirmed by mass spectrometry as well as ^{1}H and ^{13}C NMR.

Preparation and Characterization of NPs. Particle size and zeta potential measurements performed on the NPs used in this study are summarized in Table 1. As expected, no significant differences in zeta potential between bare PLA and PLA-SEL$_{5\%}$ NPs were observed due to the low concentration of synthetic ligand in the NPs. The negative surface charge of the NPs is mostly due to the remnant carboxylic groups of PLA.

NP Surface Characterization. We used TOF-SIMS to detect the presence of the ligand directly on the surface of the NPs. For these experiments, no fluorescently labeled polymers were used. Excipients coming from NP preparation and polymers used did not contain any nitrogen atoms. TOF-SIMS is a very surface-specific technique and sensitive to the outermost 10 Å of the NP surface. In Figure 2, the 40−46 amu region of the mass

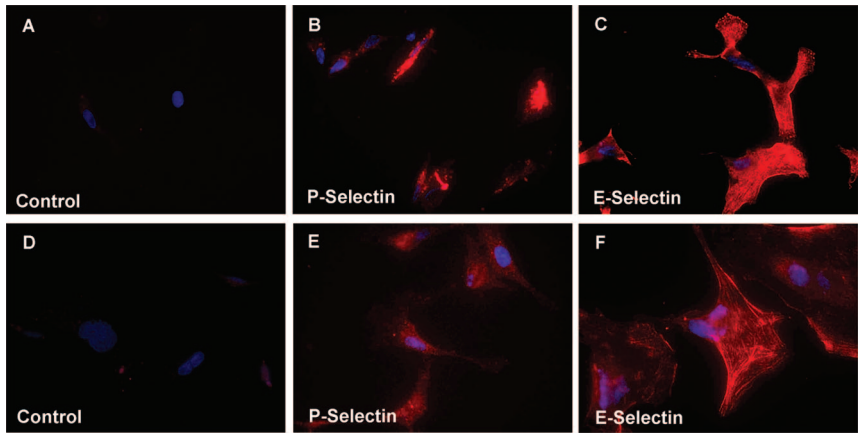

Figure 5. Fluorescent micrographs of HUVECs activated with LPS (B,C) and with L-NAME (E,F). Significant localization of fluorescence (red channel) was observed for E-selectin induced by L-NAME compared to LPS, while LPS-activated cells demonstrate higher levels of E- and P-selectin on their surfaces. Control experiments represent E-selectin (A) and P-selectin (D) expression under basal conditions. Blue channel represents nucleus staining.

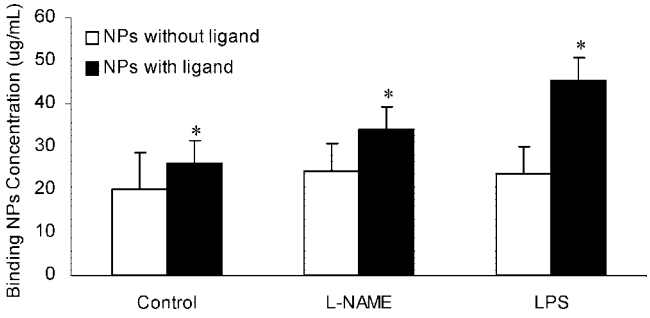

Figure 6. Fluorescence spectrophotometry demonstrates that binding of the NPs is regulated by receptor expression. The concentration of bound NPs on the cell surface was dependent on the activating molecule and was a maximum for LPS ($p < 0.01$, $n = 3$). NP binding time was 5 min at 4 °C, followed by extensive washing and cell lysis.

spectra is displayed, showing peak differences that can be attributed to nitrogen compounds found on ligand-functionalized NPs only.

NP Cytotoxicity Studies. Cytotoxicity of NPs made of PLA or PLA- $SEL_{5\%}$ was investigated *in vitro* on two different cell lines, namely, rat macrophages (Raw 264.7) and human vascular endothelial cells (Figure 3A,B). Blank experiments showed no significant polymer absorbance in the concentration range studied. Results of MTT assay demonstrated that the NPs are nontoxic in concentration lower than 100 μg/mL. Moreover, microscopic observations of the macrophage or human vascular endothelial monolayer during the study showed no changes in cell morphology or growing patterns (data not shown).

Binding Capacity of the NPs *in Vitro*. Selectin expression by HUVECs incubated with pro-inflammatory drugs was characterized by fluorescence microscopy. The relative concentration of E- and P-selectins on HUVEC surface was quantified using fluorescent anti-E-selectin and anti-P-selectins mAbs and normalized to basal concentrations on control cells (Figure 4). Upon incubation with LPS, E- and P-selectin concentrations could be enhanced 3- and 2-fold, respectively. Incubation of cells with the drug L-NAME leads to lower expression of the receptors but was still significantly higher than control cells. Fluorescence micrographs also evidenced differences in E-selectin distribution on the surface of activated cells dependently of the activating drug (Figure 5). P-selectin stained with anti-P-selectin mAbs appeared to be uniformly distributed around the cell nucleus independently of the activating drug (Figure 5B,E). E-Selectin exhibits a very different distribution pattern depending on the activating molecules. With LPS activation, a large fraction of the proteins are uniformly distributed on cell surfaces, (Figure 5C), while with L-NAME, a significant amount are clustered in filamentous structures (Figure 5F). Cytoskeletal staining with anti-F-actin mAbs was done to ensure that cell membrane permeability was not increased by formaldehyde treatment.

To determine the binding capacity of NPs to HUVECs expressing basal or high levels of selectin receptors, cells were treated with NPs for 5 min at 4 °C in order to decrease uptake by active endocytosis. After this short incubation, cells were abundantly washed and the concentration of bound NPs was quantified at 25 °C by fluorescence photospectrometry (Figure 6). For cells incubated with LPS, NPs formulated with PLA-$Sel_{5\%}$ present a 2-fold enhancement of bound concentration compared to nonactivated cells and a 30% enhancement for cells incubated with L-NAME. NPs formulated with PLA were not sensitive to expression levels of selectins and exhibit a constant but low bound NPs concentration independently of the experimental conditions. The level of NPs bearing the synthetic ligand corresponds well with the level of expression of E- and P-selectin induced by LPS and L-NAME, indicating that adhesion of these NPs is strongly dependent on selectin expression.

Fluorescent micrographs of cells activated with LPS confirmed this result. Strong fluorescence localized on the whole surface of the cell was observed after just 5 min of incubation with NPs bearing the synthetic ligand, while almost no fluorescence could be observed with the NPs formulated with PLA (Figure 7). Control experiments of F-actin staining on permeabilized and nonpermeabilized cells were also realized and confirmed that the observed fluorescence in micrographs came from cell surfaces and not from cytosol (data not shown).

Binding assay of NPs in the presence of free ligand was also realized. Free ligand was incubated for 30 min with HUVEC, which were activated with LPS or L-NAME. They were cooled to 4 °C prior to the introduction of the NPs. An increase of the free ligand concentration was followed by a decrease in the fluorescence intensity only for the NPs bearing the synthetic ligand (Figure 8). Fluorescence intensities similar to those of control cells, which were not activated or incubated with the free ligand, were obtained for free ligand concentrations higher

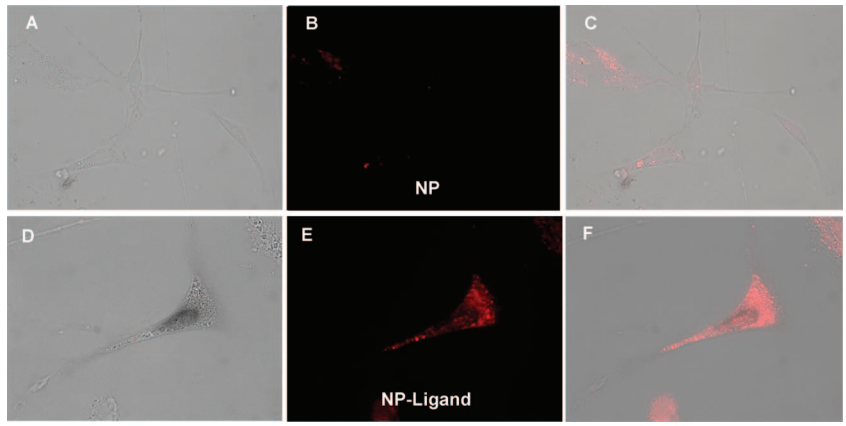

Figure 7. Fluorescent microscopy was used to assess localization of the NPs (red) on LPS activated cell surface. Images confirmed that NPs bearing ligand molecules rapidly adhere to the cell surface (E) compared to the bare NPs (B). NP binding time was 5 min at 4 °C and was followed by extensive washing and fixation of the cells. (A) and (D) are DIC images; (C) and (F) are merged images.

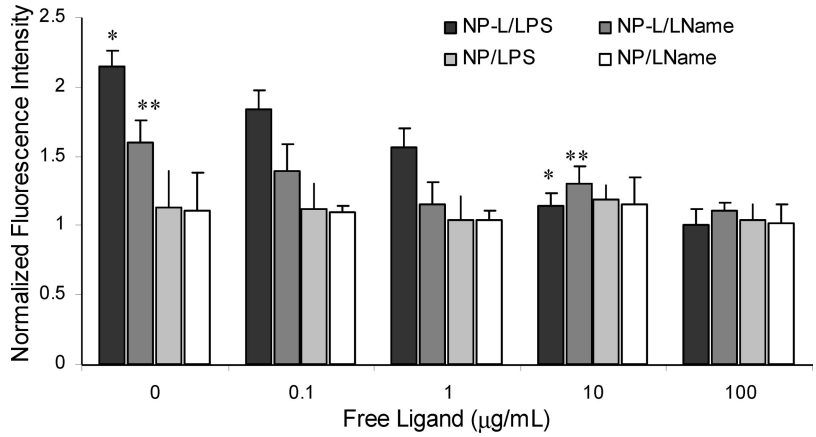

Figure 8. Fluorescence spectrophotometry demonstrated that free ligand can inhibit binding of NPs bearing ligand molecules ($p < 0.01$, $n = 3$). Binding of bare NPs was not affected. NP binding time was 5 min at 4 °C and was followed by extensive washing and cell lysis. Fluorescence intensities were normalized to control conditions (nonactivated cells treated with NPs).

than 10 μg/mL. NPs formulated with PLA were not sensitive to the presence of free ligand in the whole range of concentration studied.

DISCUSSION

The natural ligand of E- and P-selectin, the tetrasaccharide sialyl Lewis x (sLe^X), has a weak affinity (around 0.6 mM) for E-selectin as determined in cell-free assays (*25*). Development of synthetic carbohydrate ligands having higher affinities has been hindered by the fact that the synthesis of modified carbohydrate is complex and expensive. Moreover, most proteins bind carbohydrates with weak affinity. At a molecular level, X-ray diffraction analysis of E- and P-selectin (*21*) binding sites of natural ligand sLe^x had recently shown the essential chemical groups involved in the binding pocket. Consequently, several designs of antagonist ligands have been proposed (*8, 9*). Among them, carbohydrate mimetics of sLe^x based on a mannose ring have been extensively studied (*24, 26*). The advantage of these molecules is the relative ease of their synthesis and their high affinity toward E- and P-selectin. The binding pattern and conformation of the synthetic ligand grafted to a polymeric chain of PLA was evaluated and compared to the free synthetic ligand. Docking experiments performed on the free synthetic ligand showed that one of the anomeric hydroxyl functions present at the 6-O position of the α-D-mannopyranosyl ring is nonessential for the binding of the ligand. Thus, it could be possible to graft a polymeric chain at that position. The simulation results showed that grafting the synthetic ligand to a hydrophobic polymeric chain like PLA did not alter significantly the interaction pattern of the ligand with the protein. This is in agreement with previous experimental observations made by Wong et al. who showed that conjugation of hydrophobic groups like C_{16} alkyl chains on the nonessential hydroxyl group of the ligand strongly increased the affinity of the ligand to E- and P-selectin (*24*). The technique used to evaluate the NPs allows mixing of functionalized and nonfunctionalized PLA chains and offers the possibility of adjusting the concentration of ligand in the NPs. This versatility in the formulation has also allowed encapsulation of hydrophilic (*27*) or hydrophobic drugs (*28*) in PLA NPs and fine-tuning of the delivery kinetics of these drugs. An important advance of the present approach resides in the fact that, by mixing a ligand functionalized polymer with a nonfunctionalized homologue, a high concentration of ligand on the NP surface can be maintained during the whole lifetime of the NPs, contrary to NPs that are surface-functionalized only (*29*).

As already mentioned, the presence of the synthetic ligand on the NPs is a key factor to ensure strong affinity of the NPs to their target. TOF-SIMS results ensured that functionalized NPs really exposed the synthetic ligand on their surfaces. Cytotoxicity assays did not reveal any toxicity associated with NPs over a large range of NP concentrations, ensuring that binding of NPs was not affected by the chemical components of the polymers.

Under normal conditions, both E-selectin and P-selectin are present in low concentrations in vascular endothelial cells but can be induced by interleukins (IL), tumor necrosis factor-α

(TNF-α), lipopolysaccharides, endotoxins (*30*), and cytomegalovirus infection (*31*). Expression of E- and P-selectin by L-NAME has been used in model systems of ischemia or artherosclerosis, as it has been reported to inhibit the production of nitric oxide from endothelial cells. Our observation showed that the concentration and the distribution of E-selectin following L-NAME activation and LPS activation in HUVECs are very different. E- and P-selectin levels are higher on cells stimulated with LPS after 4 h of induction. Maximum expression of selectin on the cell surface has been reported to be at 4 h for both LPS and L-NAME activation (*32, 33*), suggesting that the differences observed in selectin concentration do not come from different expression kinetics. We observed marked differences in selectin distribution on endothelial cells activated by L-NAME or LPS. Scholz et al. reported a more diffuse pattern of E-selectin distribution on HUVEC cells activated by IL-β (*34*). This suggest that receptor distribution on the cell surface is strongly dependent on the stimulating molecule and therefore on the regulation process. More experiments are needed to truly characterize the effect of the protein distribution on the adhesive capacity of the NPs, but it can be advanced that this factor is expected to strongly affect the adhesive properties of the NPs as already suggested by other studies. Indeed, it has been reported that the location of the ligand−receptor bond relative to the endothelial or particle surface influences the adhesion of NPs to the endothelium (*35, 36*).

Results from *in vitro* adhesion tests demonstrated that the presence of the ligand was necessary to achieve strong adhesion between cells and NPs. Given that the NPs used in this study have the same particle size and similar zeta potentials, differences in binding properties of the NPs could be directly correlated with the presence of the ligand on NP surface. We observed that NP binding was modulated by selectin upregulation. Indeed, different levels of selectin expression could be achieved by incubating the cells with different pro-inflammatory drugs. These differences in receptor expression could be correlated with differences in binding concentrations for the NPs bearing the synthetic ligand.

In a nutshell, these results obtained *in vitro* confirm the adhesion capabilities of NPs functionalized with selectin ligand, which makes them good candidates for active targeting of the endothelium. Such findings provide important information regarding possible treatments of acute inflammation using drug delivery systems.

ACKNOWLEDGMENT

The authors want to thank NSERC and GRUM for financial support and Suzie Poulin (École Polytechnique, Université de Montréal) for TOF-SIMS analysis. J.-F. Bouchard is supported by Health Research Foundation R&D Canadian Institutes of Health Research Scholar.

LITERATURE CITED

(1) Simon, S. I., and Green, C. E. (2005) Molecular mechanics and dynamics of leukocyte recruitment during inflammation. *Annu. Rev. Biomed. Eng. 7*, 151–85.

(2) Colden-Stanfield, M., and Gallin, E. K. (1998) Modulation of K+ currents in monocytes by VCAM-1 and E-selectin on activated human endothelium. *Am. J. Physiol. 275* (1 Pt 1), C267–77.

(3) Ye, C., Kiriyama, K., Mistuoka, C., Kannagi, R., Ito, K., Watanabe, T., Kondo, K., Akiyama, S., and Takagi, H. (1995) Expression of E-selectin on endothelial cells of small veins in human colorectal cancer. *Int. J. Cancer 61* (4), 455–60.

(4) Vallien, G., Langley, R., Jennings, S., Specian, R., and Granger, D. N. (2000) Expression of endothelial cell adhesion molecules in neovascularized tissue. *Microcirculation 7* (4), 249–58.

(5) Bhaskar, V., Law, D. A., Ibsen, E., Breinberg, D., Cass, K. M., DuBridge, R. B., Evangelista, F., Henshall, S. M., Hevezi, P., Miller, J. C., Pong, M., Powers, R., Senter, P., Stockett, D., Sutherland, R. L., von Freeden-Jeffry, U., Willhite, D., Murray, R., Afar, D. E., and Ramakrishnan, V. (2003) E-selectin upregulation allows for targeted drug delivery in prostate cancer. *Cancer Res. 63* (19), 6387–94.

(6) Ehrhardt, C., Kneuer, C., and Bakowsky, U. (2004) Selectins-an emerging target for drug delivery. *Adv. Drug Delivery Rev. 56* (4), 527–49.

(7) Magnani, J. L. (2004) The discovery, biology, and drug development of sialyl Lea and sialyl Lex. *Arch. Biochem. Biophys. 426* (2), 122–31.

(8) Simanek, E. E., McGarvey, G. J., Jablonowski, J. A., and Wong, C. H. (1998) Selectin-carbohydrate interactions: from natural ligands to designed mimics. *Chem. Rev. 98*, 833–862.

(9) Kaila, N., and Thomas, B. E. t. (2002) Design and synthesis of sialyl Lewis(x) mimics as E- and P-selectin inhibitors. *Med. Res. Rev. 22* (6), 566–601.

(10) Allen, T. M., and Cullis, P. R. (2004) Drug delivery systems: entering the mainstream. *Science 303* (5665), 1818–22.

(11) Kuldo, J. M., Ogawara, K. I., Werner, N., Asgeirsdottir, S. A., Kamps, J. A., Kok, R. J., and Molema, G. (2005) Molecular pathways of endothelial cell activation for (targeted) pharmacological intervention of chronic inflammatory diseases. *Curr. Vasc. Pharmacol. 3* (1), 11–39.

(12) Everts, M., Kok, R. J., Asgeirsdottir, S. A., Melgert, B. N., Moolenaar, T. J., Koning, G. A., van Luyn, M. J., Meijer, D. K., and Molema, G. (2002) Selective intracellular delivery of dexamethasone into activated endothelial cells using an E-selectin-directed immunoconjugate. *J. Immunol. 168* (2), 883–9.

(13) Everts, M., Asgeirsdottir, S. A., Kok, R. J., Twisk, J., deVries, B., Lubberts, E., Bos, E. J., Werner, N., Mejer, D. K., and Molema, G. (2003) Comparison of E-selectin expression at mRNA and protein levels in murine models of inflammation. *Inflamm. Res. 52* (12), 512–8.

(14) Spragg, D. D., Alford, D. R., Greferath, R., Larsen, C. E., Lee, K. D., Gurtner, G. C., Cybulsky, M. I., Tosi, P. F., Nicolau, C., and Gimbrone, M. A., Jr. (1997) Immunotargeting of liposomes to activated vascular endothelial cells: a strategy for site-selective delivery in the cardiovascular system. *Proc. Nat. Acad. Sci. U.S.A. 94* (16), 8795–800.

(15) Bendas, G., Krause, A., Schmidt, R., Vogel, J., and Rothe, U. (1998) Selectins as new targets for immunoliposome-mediated drug delivery. A potential way of anti-inflammatory therapy. *Pharm. Acta Helv. 73* (1), 19–26.

(16) Kessner, S., Krause, A., Rothe, U., and Bendas, G. (2001) Investigation of the cellular uptake of E-Selectin-targeted immunoliposomes by activated human endothelial cells. *Biochim. Biophys. Acta 1514* (2), 177–90.

(17) Murohara, T., Margiotta, J., Phillips, L. M., Paulson, J. C., DeFrees, S., Zalipsky, S., Guo, L. S., and Lefer, A. M. (1995) Cardioprotection by liposome-conjugated sialyl Lewisx-oligosaccharide in myocardial ischaemia and reperfusion injury. *Cardiovasc. Res. 30* (6), 965–74.

(18) Vodovozova, E. L., Moiseeva, E. V., Grechko, G. K., Gayenko, G. P., Nifant'ev, N. E., Bovin, N. V., and Molotkovsky, J. G. (2000) Antitumour activity of cytotoxic liposomes equipped with selectin ligand SiaLe(X), in a mouse mammary adenocarcinoma model. *Eur. J. Cancer 36* (7), 942–9.

(19) DeFrees, S. A., Phillips, L., Guo, L., and Zalipsky, S. (1996) Sialyl Lewis x liposomes as a multivalent ligand and inhibitor of E-selectin mediated cellular adhesion. *J. Am. Chem. Soc. 118* (26), 6101–6104.

(20) Jones, G., Willett, P., and Glen, R. C. (1995) Molecular recognition of receptor-sites using a genetic algorithm with a description of desolvation. *J. Mol. Biol. 245* (1), 43–53.

(21) Somers, W. S., Tang, J., Shaw, G. D., and Camphausen, R. T. (2000) Insights into the molecular basis of leukocyte tethering and rolling revealed by structures of P- and E-selectin bound to SLe(X) and PSGL-1. *Cell 103* (3), 467–79.

(22) Jones, G., Willett, P., Glen, R. C., Leach, A. R., and Taylor, R. (1997) Development and validation of a genetic algorithm for flexible docking. *J. Mol. Biol. 267* (3), 727–748.

(23) Nadeau, V., Leclair, G., Sant, S., Rabanel, J. M., Quesnel, R., and Hildgen, P. (2005) Synthesis of new versatile functionalized polyesters for biomedical applications. *Polymer 46* (25), 11263–11272.

(24) Wong, C. H., MorisVara, F., Hung, S. C., Marron, T. G., Lin, C. C., Gong, K. W., and WeitzSchmidt, G. (1997) Small molecules as structural and functional mimics of sialyl Lewis X tetrasaccharide in selectin inhibition: A remarkable enhancement of inhibition by additional negative charge and/or hydrophobic group. *J. Am. Chem. Soc. 119* (35), 8152–8158.

(25) Weitz-Schmidt, G., Gong, K. W., and Wong, C. H. (1999) Selectin/glycoconjugate binding assays for the identification and optimization of selectin antagonists. *Anal. Biochem. 273* (1), 81–8.

(26) Marron, T. G., Woltering, T. J., WeitzSchmidt, G., and Wong, C. H. (1996) C-Mannose derivatives as potent mimics of sialyl Lewis X. *Tetrahedron Lett. 37* (50), 9037–9040.

(27) Hammady, T., Nadeau, V., and Hildgen, P. (2006) Microemulsion and diafiltration approaches: An attempt to maximize the global yield of DNA-loaded nanospheres. *Eur. J. Pharm. Biopharm. 62* (2), 143–154.

(28) Sant, S., Thommes, M., and Hildgen, P. (2008) Microporous structure and drug release kinetics of polymeric nanoparticles. *Langmuir 24* (1), 280–287.

(29) Eniola, A. O., and Hammer, D. A. (2005) Characterization of biodegradable drug delivery vehicles with the adhesive properties of leukocytes II: effect of degradation on targeting activity. *Biomaterials 26* (6), 661–70.

(30) Fries, J. W. U., Williams, A. J., Atkins, R. C., Newman, W., Lipscomb, M. F., and Collins, T. (1993) Expression of Vcam-1 and E-Selectin in an in-Vivo Model of Endothelial Activation. *Am. J. Pathol. 143* (3), 725–737.

(31) Scholz, M., Hamann, A., Blaheta, R. A., Auth, M. K. H., Encke, A., and Markus, B. H. (1992) Cytomegalovirus-related and interferon-related effects on human endothelial-cells - cytomegalovirus-infection reduces up-regulation of HLA class-II antigen expression after treatment with interferon-gamma. *Hum. Immunol. 35* (4), 230–238.

(32) Leeuwenberg, J. F. M., Smeets, E. F., Neefjes, J. J., Shaffer, M. A., Cinek, T., Jeunhomme, T., Ahern, T. J., and Buurman, W. A. (1992) E-Selectin and intercellular-adhesion molecule-1 are released by activated human endothelial-cells invitro. *Immunology 77* (4), 543–549.

(33) Armstead, V. E., Minchenko, A. G., Schuhl, R. A., Hayward, R., Nossuli, T. O., and Lefer, A. M. (1997) Regulation of P-selectin expression in human endothelial cells by nitric oxide. *Am. J. Physiol. 273* (2), H740–746.

(34) Scholz, D., Devaux, B., Hirche, A., Potzsch, B., Kropp, B., Schaper, W., and Schaper, J. (1996) Expression of adhesion molecules is specific and time-dependent in cytokine-stimulated endothelial cells in culture. *Cell Tissue Res. 284* (3), 415–23.

(35) Patel, K. D., Nollert, M. U., and McEver, R. P. (1995) P-selectin must extend a sufficient length from the plasma membrane to mediate rolling of neutrophils. *J. Cell Biol. 131*, 1893–1902.

(36) Schaffer, D. V., and Lauffenburger, D. A. (1998) Optimization of cell surface binding enhances efficiency and specificity of molecular conjugate gene delivery. *J. Biol. Chem. 273* (43), 28004–28009.

BC800257M